6. Chemical Contributions to Extinction

This section estimates the contribution from the major chemical components of light scattering and absorption and examines how these contributions vary from site to site and time to time throughout the Project MOHAVE network.

6.1 Median and Maximum Concentrations of Chemical Components over the Study Region

Table 6-1 through Table 6-4 show the median and maximum aerosol concentrations over the Project MOHAVE network during both the winter and summer intensive sampling periods. The chemical species headings for these tables are defined in Table 6-5. The median concentrations are presented here instead of the average concentrations because median values are insensitive to biases introduced when less than half of the samples are below the lower detectable limit. When median values are shown as 0 in Table 6-1 and Table 6-3, more than 50% of the samples collected were below the lower detectable limit of the analysis.

During the winter months, the highest median levels of fine mass were distributed throughout the network at Cajon Pass (4.7 $\mu g/m^3$), Las Vegas Wash (5.9 $\mu g/m^3$), and Marble Canyon (4.7 $\mu g/m^3$). However, in the summer months, the highest median fine mass concentrations were recorded on the western edge of the network at Cajon Pass (17 $\mu g/m^3$), San Gorgonio (11 $\mu g/m^3$), and Tehachapi Pass (11 $\mu g/m^3$).

Fine particulate trace element concentrations used for chemical mass balance modeling displayed strong spatial gradients over the sampling area. Median wintertime selenium concentrations at Marble Canyon were 4 times greater than the next highest site in the network. The highest median wintertime concentrations of zinc and manganese were observed at Las Vegas Wash. Summertime bromine concentrations were highest on the southwestern edge of the network at Cajon Pass, Barstow, El Centro, and San Gorgonio. Also, median potassium levels were highest at El Centro during the summer.

In addition to the XRF analysis, elemental and organic carbon analysis were performed on samples collected at the Bryce Canyon, Hopi Point, Indian Gardens (wintertime only), Joshua Tree, Meadview, Petrified Forest, San Gorgonio, Sycamore Canyon, and Tonto. For the winter and summer intensive periods at these sites, the average concentrations of the components of the fine mass in the study region were calculated with the equations described by Sisler et al. (1996).

$$[(NH_4)_2SO_4] = 4.125\,S \qquad (6\text{-}1)$$

$$[NH_4NO_3] = 1.29\,NO_3 \qquad (6\text{-}2)$$

$$[OMC] = 1.4\,OC \qquad (6\text{-}3)$$

$$[EC] = EC \qquad (6\text{-}4)$$

$$[Soil] = 2.2\,Al + 2.19\,Si + 1.63\,Ca + 2.42\,Fe + 1.94\,Ti \qquad (6\text{-}5)$$

Table 6-1 Median aerosol concentrations from the Project MOHAVE wintertime intensive sampling period (1/14/92 – 2/15/92). Concentrations are reported in ng/m^3 except for BAP which has units of 10^{-8} m^{-1}.

SITE	AMBO	BAKE	BRCA	CAJO	COCO	DARO	DOSP	HOP5	HOPO	HUMO	ING5	INGA	JALA	JOT2	JOTR	LVWA	MACN	MED5	MED6	MOSP	NEHA	OVBE	PARK	PAUL	PEFR	SAGR	SELI	SPMO	SQMO	SYCA	TEHA	TONT	TRUX	WICK	YUCC
MF	2300	3700	1100	4700	2800	3700	2200	1500	1500	940	2800	2900	1100	3800	3500	5900	4700	1600		1300	1800	3500	4300	3600	3600	1200	2600	1500	1400	2800	2900	3000	3600	2800	3500
BAP	540	1200	200	1200	600	660	420	270	260	160	460	460	160	490	480	1400	880	350		180	360	720	900	730	880	270	510	330	230	640	450	560	560	520	620
M10			2500					6100			7500				11000			3900							7100	2900				6100		6600			
H	72	110	46	130	93	140	78	62	58	43	100	110	44	77	80	190	180	90		45	69	130	130	120	150	48	120	76	61	120	90	140	120	120	110
NA	0	0	0	0	0	13	0	10	0	9	9.6	0	0	0	0	0	11	0		12	0	12	20	15	0	0	0	0	0	0	0	0	0	5.2	0
MG	0	0	0	0	0	0	0	0	0	0	0	0	0	0	0	39	0	0		0	0	0	0	0	0	0	0	0	0	0	0	0	0	0	0
AL	0	67	0	71	0	0	36	0	0	0	0	1.5	0	110	100	0	25	0		0	0	14	49	0	0	0	0	0	0	0	0	0	42	0	37
SI	74	170	21	170	52	50	74	28	30	24	54	45	22	230	230	130	67	37		35	25	130	120	41	53	30	42	38	25	64	54	38	180	39	110
P	0	0	0	0	0	0	0	0	0	0	0	0	0	0	0	0	0	0		0	0	0	0	0	0	0	0	0	0	0	0	0	0	0	0
S	140	160	110	170	190	300	190	150	170	110	250	250	85	130	120	220	440	200		94	140	250	230	180	260	66	190	160	120	140	100	270	170	210	210
CL	0	0	0	0	0	0	0	0	0	0	0	0	0	0	0	0	0	0		0	0	0	0	0	0	0	0	0	0	0	0	0	0	0	0
K	18	33	5.6	37	13	12	15	6.8	7.1	6.2	11	9.3	6	41	45	39	15	11		8.5	9.2	23	35	15	9.2	8.9	11	9.7	5.7	18	13	10	35	14	21
CA	38	64	6.8	44	31	14	30	11	10	7.6	19	18	6.5	41	37	150	22	17		39	11	57	59	21	16	9.2	14	19	8.9	14	16	9.4	220	10	56
TI	6.1	8.6	1.9	6.6	2.7	3.9	5.3	4.3	1.2	1.4	3.3	2.3	2.9	5.5	4.6	5.7	5.7	3.1		4.7	1.2	4.2	4.7	1.7	3.3	0	1.1	0.8	0.5	1.4	0.9	0.47	3.2	0.5	1.7
V	0	0	0	0	0	0	0	0	0	0	0	0	0	0	0	0	0	0		0	0	0	0	0	0	0	0	0	0.34	0	0	0.4	0	0	0
CR	0	0	0.28	0	0	0	0	0	0	0	0	0	0	0	0	0	0	0		0	0	0	0	0	0	0.28	0.14	0.27	0.34	0	0	0	0	0	0
MN	0.75	1.6	0.36	2	1	0.5	0.77	0.36	0.26	0.39	0.49	0.34	0	1.6	1.5	5.4	0.58	0.5		0.58	0.48	0.73	1.3	0.73	0.62	0.46	0.73	0.55	0.44	0.76	0.55	0.61	1.6	0.67	1.2
FE	25	46	3.6	83	17	13	21	7.2	7.2	6.6	9.8	9.2	4.6	41	43	44	17	8.8		9.3	8.5	28	32	15	16	7.9	16	11	8.2	23	14	8.9	48	8.5	32
NI	0	0	0	0	0	0	0	0	0	0	0	0	0	0	0	0	0	0		0	0	0	0	0	0	0	0	0	0	0	0	0	0	0	0
CU	0.54	0.72	0.15	0.97	0.69	3.3	0.34	1.4	1.1	0.4	0.66	0.62	0.13	0.29	0.35	1.8	0.4	1.4		0.38	1.5	0.9	0.64	0.39	0.42	0.44	0.49	2.6	0.29	0.72	0.37	2.5	0.34	1.4	0.78
ZN	2	2.7	0.49	3	1.7	1.8	1.1	0.98	0.8	0.72	0.93	0.93	0.51	1.3	1.5	3.7	1.5	0.75		0.87	1.4	2.2	2.4	1.2	1.3	0.74	1.4	1.2	0.85	1.5	1.5	2.1	1.1	2.2	1.5
AS	0	0	0	0.25	0	0	0	0	0	0	0	0	0	0.12	0	0	0	0		0	0.16	0	0	0	0	0	0	0	0	0	0.15	0.15	0	0	0
PB	0.77	1	0.23	0.79	0.85	0.59	0.62	0.27	0.32	0.29	0.33	0.46	0.27	0.55	0.76	1.9	1.3	0.37		0.43	0.52	0.9	3.8	0.66	0.56	0.34	0.54	0.42	0.36	0.39	0.6	1.4	0.54	1.2	0.76
SE	0.19	0.16	0.09	0.16	0.4	0.47	0.29	0.19	0.18	0.08	0.37	0.42	0.11	0.09	0.035	0.34	2	0.24		0.09	0.26	0.58	0.44	0.28	0.43	0	0.25	0.24	0.14	0.15	0.05	0.32	0.23	0.21	0.31
BR	1.3	1.6	0.56	1.4	1.2	1.2	1.1	0.63	0.69	0.49	0.9	0.94	0.55	0.94	1	1.8	1.6	0.84		0.79	1.2	1.5	2.5	1.1	0.97	0.6	1	0.83	0.68	0.75	0.96	0.73	1	1.1	1.2
RB	0.41	0.85	0	0.42	0.36	0.34	0.42	0	0	0	0	0	0	0.51	0.43	0.65	0	0		0.43	0.34	0.35	0	0.39	0	0	0	0.17	0	0	0	0	0.69	0	0.48
SR	0.45	0.78	0.15	0.59	0.64	0.29	0.45	0.2	0.14	0.15	0.29	0.31	0.18	0.52	0.51	1.7	0.71	0.23		0.35	0	0.8	0.86	0.18	0.24	0.16	0.25	0.26	0.14	0.23	0.26	0.21	0.73	0.18	0.59
ZR	0	0	0	0.19	0	0	0	0	0	0	0	0	0	0.25	0	0	0	0		0	0	0.47	0	0	0	0	0	0	0	0	0	0	0	0	0
MO	0	0	0	0	0	0	0	0	0	0	0	0	0	0	0	0	0	0		0	0	0	0	0	0	0	0	0	0	0	0	0	0	0	0
BSO4			380					550			750				420			640	530						820	220				510		1100			
CLM			7.9					5.8			1.9				30			0	1.5						7.7	14				4.3		10			
NO2M			16					27			20				8.9			20	0						25	1.9				24		18			
NO3M			110					65			96				200			79	9.1						220	230				170		150			
NH4I																			180																
NH3I																			94																
SO2I10			120					670			590				120			110							640	90				270		480			
SO2I25	380	930		760	690		360			310			470			890	5500			200	320	620	1800	130			190	450	330		220		180	490	820
OCLT			0					26			45				34			19							0	29				6.1		0			
OCHT			86					290			490				390			540							670	360				540		570			
ECLT			0					7.2			23				29			6.3							170	43				56		80			
ECHT			19					90			120				85			89							220	75				140		88			

Table 6-2 Maximum aerosol concentrations from the Project MOHAVE wintertime intensive sampling period (1/14/92 – 2/15/92). Concentrations are reported in ng/m^3 except for BAP which has units of 10^{-8} m^{-1}.

SITE	AMBO	BAKE	BRCA	CAJO	COCO	DARO	DOSP	HOP5	HOPO	HUMO	ING5	INGA	JALA	JOT2	JOTR	LVWA	MACN	MED5	MED6	MOSP	NEHA	OVBE	PARK	PAUL	PEFR	SAGR	SELI	SPMO	SQMO	SYCA	TEHA	TONT	TRUX	WICK	YUCC
MF	4900	5700	3400	19000	5500	5400	4800	3900	3400	2600	8200	4800	3600	7300	6500	9400	12000	4300		4200	8700	5000	8400	5700	7200	15000	4900	3800	7300	8400	10000	9800	7000	7300	6300
BAP	1000	2100	630	1800	890	1000	1100	760	710	480	990	840	630	1100	950	2600	1800	720		760	1100	1300	2400	1200	1700	960	1100	670	1200	1500	1400	940	1000	960	1300
M10			10000					35000			24000				30000			13000							17000	17000				13000		14000			
H	180	200	210	750	210	240	170	140	130	130	360	190	190	210	190	340	540	180		170	360	220	280	240	330	700	200	170	160	460	440	430	200	340	260
NA	120	83	22	120	92	64	66	66	89	50	93	63	40	120	130	84	53	140		64	38	59	150	57	53	60	34	50	83	70	180	62	73	63	79
MG	54	26	12	32	32	9.2	13	31	10	15	22	0	25	21	21	120	8	21		21	15	0	9.9	9.4	21	21	15	25	19	15	33	22	34	21	11
AL	150	170	44	310	91	15	100	36	41	21	50	61	46	530	400	130	150	80		95	43	82	200	70	50	68	100	56	23	93	80	34	320	44	110
SI	340	440	89	710	140	140	210	99	90	95	120	95	66	840	760	370	230	160		170	82	200	380	150	140	160	200	120	310	190	350	120	610	110	230
P	45	0	2.6	0	0	0	0	2.5	0	7	0	0	0	0	0	0	0	0		2.8	0	0	0	0	0	3.7	0	2.3	8	0	2.7	0	0	0	0
S	500	380	380	620	420	710	380	420	340	340	1100	590	450	540	550	440	1700	450		370	690	420	660	420	830	560	430	390	310	330	480	640	360	430	430
CL	29	0	1.5	0	0	0	1.2	1.4	1.2	5.2	1.7	0	0	0	1.3	0	1.8	15		2.6	2.1	0	18	4.6	0	1.5	1.7	1.1	3.3	0	79	0	0	0	34
K	51	72	20	120	30	21	43	20	15	16	20	19	17	140	120	71	33	36		38	24	73	110	35	26	39	29	26	31	38	56	52	130	37	99
CA	170	140	20	180	110	31	93	26	41	22	74	60	25	140	130	430	74	40		92	22	150	250	58	22	47	49	44	710	41	91	21	660	27	130
TI	11	15	3.5	16	6.5	5.6	9.5	7	2.3	4.4	8.2	4.4	5.3	16	15	11	11	6.4		6.9	3.4	10	9.5	4.1	7.2	1.9	7.3	2	3.1	5.4	4.7	3.9	7.7	1.3	5.3
V	1.2	1.2	0	2	0.78	0	1.4	1	0.43	1.4	1.9	0.45	1.3	1.3	0.9	1.6	0.76	1.5		1.2	0.74	1.6	0.62	1.1	1.8	1.3	0.71	0.79	0.92	0.95	1.9	0.97	1.1	0.95	0.95
CR	0.68	0.75	0.65	0.85	0.47	0.57	0.94	2.4	1.4	1.3	1	0.36	0.66	0.36	0.92	0.93	1.1	0.84		0.79	0.67	1.3	1	0.93	0.98	0.91	0.86	1.1	1.1	1	0.68	0.83	0.7	0.64	0.65
MN	2.8	4.1	1	6.3	2.3	1.3	2	0.88	0.7	1.1	1.7	1	1.2	5.8	5.1	15	1.4	1.6		2.2	1.2	1.9	4	1.7	1.6	1.7	2.1	1.1	2.3	3	2.6	8.9	4.3	1.5	4.1
FE	97	94	14	180	44	39	57	32	21	22	42	24	17	130	130	95	60	62		44	21	47	79	41	39	34	82	25	68	91	62	75	120	23	74
NI	0.25	0	0	0.34	0.5	0.74	0.36	0.81	1.2	0.49	0.54	0.81	0.1	0.35	0.32	2.3	0.53	0.25		0.16	0.14	0.52	0.22	0.17	0	0.16	0.49	0	0.33	0.15	1.8	0.08	0	0.22	0.17
CU	4.6	25	1.8	2.8	3	54	2.8	25	5.5	1.9	11	4.1	1.7	1.6	1.8	10	2.3	20		6.2	13	6.6	5.4	1.7	1.9	3.4	3.5	6.1	2.4	1.7	13	16	6.7	4.3	5.3
ZN	11	24	3.8	11	3.4	41	4.9	3.8	2.1	3.5	3	1.8	2.7	12	14	6.2	2.7	6		6.6	9	3.9	6.9	4.7	11	7.2	6.4	3.3	5.4	4.4	11	6.4	6.7	5.7	6.8
AS	1	0.5	1.3	1.8	0.51	0.21	0.83	0.49	0.18	0.57	0.7	0.29	0.38	2.5	3	0.7	0.16	1.2		0.9	1.2	0.85	1.1	1.1	2.7	3.2	0.97	0.47	0.77	0.74	0.55	1.1	1	1.6	0.77
PB	1.8	3.6	2	3.3	2.6	2	3.7	1.4	1.2	2.9	1.4	1.2	1.9	2	2.1	4.8	3.8	4		2.3	3.4	7	25	4.1	1.4	1.8	4.3	2.9	4.4	3.2	3.1	4.8	4.6	5.8	3.9
SE	1.1	0.4	0.74	0.36	0.85	2.8	1	1.1	0.67	0.32	2.3	1.9	1.8	0.23	0.27	0.67	15	0.73		1.2	0.91	1.1	1.4	0.68	1.1	0.27	0.83	0.53	0.44	0.38	0.47	0.77	0.66	0.49	0.74
BR	2.2	2.7	1.8	2.4	3.1	1.5	2.7	2.1	1.2	1.4	1.6	1.5	2.3	3.3	2.7	2.6	2.7	4.1		1.9	6.7	3.7	11	2.5	1.5	1.7	1.9	2.5	1.2	1.4	2.2	1.2	2	1.5	2.5
RB	1.7	1.6	0.71	1.6	1.2	0.64	0.79	0.62	0.48	0.73	0.76	0.73	0.88	1.9	2	1.4	1.4	0.41		1	1	0.86	0.97	1.1	0.41	0.57	0.88	1.2	0.83	0.37	0.81	0.44	1.7	0.9	1.5
SR	3.2	2.4	0.31	3.2	2.2	0.85	4.7	1.7	0.35	0.43	0.99	1	0.82	3.9	4	3	2.5	1.9		2.7	0.32	2.3	1.9	0.51	0.53	2.7	0.76	0.56	1.8	0.67	1.4	0.34	1.6	0.43	1.4
ZR	1.2	2.3	0.95	1.2	1.3	1.4	1.3	0.91	0.33	1.3	1.1	0.95	0.91	0.97	0.81	1.8	2.2	1.1		1.9	0.71	1.9	1.1	0.79	1.2	1.3	1	1	1.5	1.1	0.93	0.73	1.7	0.91	1.4
MO	3.5	4.6	2.2	2.3	1.2	0.75	2	1.9	0.31	2.9	2.7	0.55	2.2	0.56	1.5	1.6	3.3	2.1		4.4	1.1	2.1	2.2	1.4	2.6	1.7	1.2	0.84	0	0.98	1.4	0.83	3	0.47	1.3
BSO4			1200					1200			3100				1700			1400	1300						2500	1800				1100		2300			
CLM			36					220			140				140			72	17						35	130				80		62			
NO2M			48					110			46				27			82	160						72	31				44		51			
NO3M			2200					470			570				3100			620	190						820	7500				650		3600			
NH4I																			420																
NH3I																			440																
SO2I10			1100					5400			5700				640			2600							2200	1000				1000		3800			
SO2I25	6100	2300		1300	12000		4000			1200			12000			3400	100000			640	1200	1200	3700	500			2200	7200	2500		650		1200	1900	2900
OCLT			82					270			350				150			120							220	180				520		140			
OCHT			420					930			1200				1000			970							1800	820				3800		1000			
ECLT			41					260			220				110			180							540	280				490		240			
ECHT			130					280			320				220			290							490	190				440		200			

Table 6-3 Median aerosol concentrations from the Project MOHAVE summertime intensive sampling period (7/12/92 – 9/2/92). Concentrations are reported in ng/m^3 except for BAP which has units of 10^{-8} m^{-1}.

SITE	BAKE	BARS	BRCA	CAJC	CAJO	CIBO	COCO	DECE	DOSP	ELCE	ESSE	HOP5	HOPO	JOTR	KELS	KING	LVWA	MED5	MED6	MOSP	NEHA	OVBE	PARK	PEFR	SAGR	SELI	SPMC	SPMO	SQMO	SYCA	TEHA	TONT	TRUX	WICK	YUCC
MF	9700	10000	4300	17000	17000	6400	7300	8200	5600	10000	7500	4400	4100	9000	7000	5500	7500	5400		5700	4600	6300	7500	4900	11000	4600	5200	5300	4000	6700	11000	6100	6200	5300	5900
BAP	1700	1700	590	3000	3000	920	870	1300	720	1700	1300	650	640	1300	1100	720	1200	680		830	590	790	1100	1000	1600	650	700	700	570	790	1600	810	830	680	820
M10			8100									12000		19000				14000						7700	21000					17000		15000			
H	290	340	130	570	550	170	200	230	150	220	200	140	130	260	210	160	210	170		170	150	170	180	170	420	160	180	160	140	210	380	210	160	160	170
NA	0	0	0	0	0	0	0	0	0	0	0	0	0	0	0	0	0	0		0	0	0	0	0	0	0	0	0	0	0	0	0	0	0	0
MG	0	0	0	0	0	0	0	0	0	0	0	0	0	0	0	0	0	0		0	0	0	0	0	0	0	0	0	0	0	0	0	0	0	0
AL	0	0	0	0	0	0	0	0	0	0	0	0	0	0	0	0	0	0		0	0	0	0	0	0	0	0	0	0	0	0	0	0	0	0
SI	440	250	85	190	210	220	240	200	240	550	280	84	72	200	170	160	270	150		170	140	190	350	120	150	130	140	130	90	160	370	140	320	140	220
P	0	0	0	0	0	0	0	0	0	0	0	0	0	0	0	0	0	0		0	0	0	0	0	0	0	0	0	0	0	0	0	0	0	0
S	660	760	360	1200	1200	640	620	750	550	840	650	380	370	740	640	530	700	520		500	460	580	590	450	720	370	540	550	410	380	620	480	460	490	510
CL	0	0	0	0	0	0	0	0	0	0	0	0	0	0	0	0	0	0		0	0	0	0	0	0	0	0	0	0	0	0	0	0	0	0
K	100	70	21	59	60	76	51	79	51	200	62	21	21	57	50	41	62	35		40	38	47	95	24	41	27	40	40	25	32	110	30	60	42	52
CA	140	74	31	54	55	73	90	60	71	200	76	21	20	47	41	52	140	53		56	44	65	210	26	35	31	40	42	24	28	76	32	290	43	100
TI	11	6.4	1.7	6.7	6.9	4	5.7	4	6.4	7.1	5.5	1.8	1.6	5.1	4.4	2.8	6.2	3.1		3.4	2.4	3.4	5.2	2.5	4.3	3.8	3	2.8	1.7	5.5	9.7	3.2	5.8	2.6	3.3
V	0	0	0	0	1.3	0	0	0	0	1.9	0	0	0	0	0	0	0	0		0	0	0	0	0	0	0	0	0	0	0	0	0	0	0	0
CR	0	0	0	0	0	0	0	0	0	0	0	0	0	0	0	0	0	0		0	0	0	0	0	0	0	0	0	0	0	0	0	0	0	0
MN	0.98	0	0	0	0	0	0	0	0	0	0	0	0	0	0	0	1.1	0		0	0	0	0	0	0	0	0	0	0	0	0	0	0	0	0
FE	110	70	16	95	95	42	55	51	54	100	99	20	16	52	47	33	55	34		36	28	41	68	29	48	43	34	31	21	58	110	31	74	33	48
NI	0	0.2	0	0	0.35	0.17	0	0	0	0.55	0	0	0	0.18	0	0	0	0		0	0	0	0	0	0.26	0	0	0	0	0	0	0	0	0	0
CU	1.4	1.2	0.37	2.1	1.8	0.64	0.96	0.94	0.78	1	0.87	1.2	1.3	0.77	1	0.6	1.2	1.2		0.71	0.6	0.71	0.54	0.74	1.1	0.57	1.1	1.2	0.7	1.4	1.9	3.2	0.6	0.86	0.41
ZN	3.5	3.7	0.83	9.8	9	2	1.9	2.7	1.5	3.6	2.2	0.97	1.1	2.8	2.2	1.3	2.8	1.3		1.6	1.2	1.6	1.9	1.1	4.8	1.2	1.6	1.6	1.1	1.4	2.7	4.4	1.4	1.7	1.3
AS	0	0	0	0	0	0.27	0	0.2	0	0	0	0	0	0	0	0.14	0	0		0	0	0.08	0.26	0	0	0	0	0	0	0	0	0.45	0	0.29	0.18
PB	1.5	1.6	0.39	3.5	3.4	0.88	0.84	1.2	0.64	2.3	0.98	0.64	0.6	1.1	1	0.61	1.2	0.74		0.63	0.48	0.76	1.8	0.47	1.6	0.51	0.64	0.64	0.49	0.58	1.5	1.9	0.64	0.88	0.6
SE	0.48	0.56	0.19	1.7	1.4	0.52	0.5	0.63	0.33	1.3	0.38	0.17	0.16	0.59	0.44	0.27	0.4	0.2		0.3	0.22	0.4	0.44	0.34	0.64	0.25	0.35	0.38	0.22	0.26	0.51	0.34	0.31	0.3	0.28
BR	3.5	4.3	1.4	5.7	5.8	2.9	2.3	3.8	1.9	5.4	2.6	1.6	1.6	3.7	3.2	1.9	2.5	1.8		2.4	1.6	2	2.8	1.4	4.2	1.4	2.2	2.4	1.4	1.4	4.5	1.4	1.9	1.7	1.9
RB	0.32	0	0	0	0	0.13	0.15	0.15	0.14	0.27	0.13	0.1	0.09	0	0.04	0.1	0.19	0.14		0.1	0.11	0.13	0.18	0	0	0	0.09	0	0	0.1	0.25	0.1	0.21	0	0.15
SR	0.8	0.47	0.21	0.57	0.55	0.39	0.81	0.46	0.43	1.1	0.45	0.21	0.19	0.37	0.34	0.3	0.93	0.38		0.34	0.27	0.47	0.95	0.23	0.35	0.19	0.3	0.35	0.2	0.28	0.48	0.22	0.55	0.24	0.4
ZR	0	0	0	0	0	0	0	0.25	0	0	0	0	0	0	0	0	0	0		0	0	0	0.24	0	0	0	0	0	0	0	0	0	0	0	0
MO	0	0	0	0	0	0	0	0	0	0	0	0	0	0	0	0	0	0		0	0	0	0	0	0	0	0	0	0	0	0	0	0	0	0
BSO4			1100									1100		2300				1500	1300					1300	2300					1200		1500			
CLM			7.3									3.9		15				7.3	4.4					0	20					12		8.1			
NO2M			0									0		0				0	0.95					0.2	0					1.7		0			
NO3M			95									100		580				130	53					110	1700					180		110			
NH4I																			450																
NH3I																			110																
SO2I10			310									150		740				610						460	510					270		890			
SO2I25	1500	2000		2300	2200	620	6800	980	1400	1900	1200				1200	890	2100			660	310	1800	500			450	1400	1300	800		2000		800	630	680
OCLT			3.4									0		50				0						21	230					31		16			
OCHT			580									500		1300				430						810	2300					980		930			
ECLT			54									48		300				18						140	490					110		95			
ECHT			56									110		86				83						180	110					210		89			

Table 6-4 Maximum aerosol concentrations from the Project MOHAVE summertime intensive sampling period (7/12/92 – 9/2/92). Concentrations are reported in ng/m^3 except for BAP which has units of 10^{-8} m^{-1}.

	BAKE	BARS	BRCA	CAJC	CAJO	CIBO	COCO	DECE	DOSP	ELCE	ESSE	HOP5	HOPO	JOTR	KELS	KING	LVWA	MED5	MED6	MOSP	NEHA	OVBE	PARK	PEFR	SAGR	SELI	SPMC	SPMO	SQMO	SYCA	TEHA	TONT	TRUX	WICK	YUCC
MF	22000	18000	7900	34000	33000	11000	18000	12000	17000	20000	17000	14000	13000	15000	11000	9000	22000	11000		10000	19000	13000	14000	7200	23000	6900	9000	9500	5900	24000	22000	14000	11000	19000	9500
BAP	3400	3500	980	4600	4700	1600	1900	2300	1700	4500	2000	2000	1800	3000	1700	1200	2300	1500		1600	2800	1600	2200	1800	3200	1200	1400	1400	950	3100	2900	1600	1400	2000	1400
M10			16000									36000		39000				48000						32000	52000					50000		48000			
H	920	540	220	1400	1300	330	400	440	640	660	500	680	560	390	440	360	690	380		340	530	340	450	260	710	280	350	380	240	1100	710	300	300	320	320
NA	550	300	75	560	350	650	380	680	510	1000	510	190	100	980	640	330	580	620		390	0	380	690	0	130	0	310	340	0	240	0	0	0	410	430
MG	0	0	54	27	110	130	0	260	170	140	84	77	84	190	120	180	310	230		170	120	140	200	66	99	110	140	48	100	120	310	100	130	230	180
AL	670	430	70	220	210	230	330	380	310	490	370	110	50	220	99	140	140	250		200	50	210	480	160	150	230	99	170	52	900	390	960	600	2000	200
SI	1300	890	190	430	400	470	1000	670	580	1100	690	230	140	480	450	370	850	460		480	330	500	1200	390	280	510	290	300	270	1600	810	1700	1200	3300	500
P	0	0	0	0	0	0	0	0	0	0	0	0	0	0	0	0	0	0		0	0	0	0	0	0	0	0	0	0	0	0	0	0	0	0
S	1400	1500	720	2900	2900	990	1700	1400	1500	1400	1500	790	740	1400	1100	1200	1700	1600		1200	1600	1000	1700	660	1600	680	1500	1500	710	660	1200	1100	960	790	1200
CL	70	0	0	6.1	130	660	250	530	220	730	350	5.3	6	5.9	220	150	160	220		93	82	340	530	3.5	0	2	230	210	0	0	0	6.5	0	0	280
K	230	170	73	150	160	400	150	370	140	530	120	62	39	270	99	100	140	130		94	69	120	320	60	140	67	120	110	90	150	310	240	190	440	150
CA	510	250	67	92	100	130	440	180	160	420	230	83	47	160	140	130	400	180		170	130	210	590	57	67	120	89	92	82	150	190	260	1100	470	310
TI	25	19	3.9	17	14	7.5	22	13	13	17	12	5.7	3.8	13	8.9	6.5	20	14		9.8	7.7	13	19	7.3	56	29	7.2	8.5	5.7	81	30	38	22	56	11
V	3.5	3.2	0.95	7.1	6	2.2	1.8	2.9	1.4	9.2	1.3	1.5	1.3	4.2	1.5	1.8	2.2	2.5		1.7	2.6	1.3	1.6	1.2	2.2	1.3	1.7	2.4	2.3	4.6	2.7	1.6	2.8	1.5	1.9
CR	1.9	0.64	1	0.9	1.5	0.74	0.7	0.47	0.63	2.7	0.87	0.97	0.69	1.2	0.94	0.92	0	0.85		0	0.68	1	1.5	1	1.1	0.69	1.3	0.95	0.71	0.95	1.1	1	0.98	0.71	1.1
MN	6	2.8	0.71	3	2.8	1.9	1.6	2.3	1.6	3.2	3.5	0.97	0.87	1.5	1.6	1.3	6	1.7		1.4	1.2	1.1	5.5	1.1	2.6	3.3	1.2	1.3	1.3	11	4.8	10	3.2	14	2.1
FE	280	190	38	200	190	92	210	150	140	210	210	56	54	96	90	75	160	110		110	64	120	200	78	86	180	63	63	55	630	240	410	230	570	97
NI	0.44	0.6	0.33	1.8	1.4	0.39	0.38	0.85	0.5	3.9	0.5	0.37	0.7	0.47	0.43	0.26	2.3	1.7		0.22	0.36	0.65	0.47	0	0.95	0.32	0.38	0.48	0.3	0.23	0.32	0.57	0.23	0.29	0.59
CU	8	7.7	2.3	6.1	4.2	5.5	19	4.6	2.9	4.6	4.3	17	10	2.6	5.3	2.2	7.5	11		3.4	4.3	3.7	2.4	2	14	7.2	4.6	4.2	5.5	11	7.5	11	1.9	11	3
ZN	7.1	8.1	1.7	17	17	4.5	13	6.6	4.2	21	6.6	3.3	3.1	6.5	4.4	3.8	9.3	5.6		3.3	4.2	4.4	4.3	3.4	9	9.8	3.8	4.2	4.4	3.7	27	44	3.8	7.4	3.6
AS	0.59	0.5	0.33	0	0.55	0.73	0.79	0.77	0.72	2.5	0.73	0.53	0.32	0.62	0.58	0.76	0.63	0.84		0.66	0.52	0.72	1	1.4	0.51	0.74	0.58	0.69	0.68	0.82	0.42	2.1	1	1.8	1
PB	2.4	3.3	1.1	6	5.1	2.2	1.6	1.8	1.7	8.6	2.4	1.2	1.4	1.7	1.8	1.5	4	1.7		1.2	1.7	1.4	31	1.8	2.6	1.7	1.4	1.3	1.5	2.2	4.2	12	1.5	2.5	1.4
SE	0.94	1.1	0.48	2.7	2.4	1	1.3	1.1	0.82	2.2	0.8	0.41	0.31	1.1	0.76	0.53	0.72	0.48		0.55	0.57	0.93	1.6	0.83	1.2	0.49	0.88	0.75	0.5	0.52	0.93	0.67	0.72	0.5	0.47
BR	5.7	9.4	3.6	11	12	6.1	8	8.9	7.3	10	7.1	5.3	4.3	8.5	7.9	6.9	5.7	6.8		4.7	4.5	5.4	6.5	3.3	8.7	3.7	7.9	7.5	4	4	8.2	4	5.2	4.6	5.8
RB	0.83	0.49	0.2	0.45	0.48	0.29	0.58	0.47	0.29	0.65	0.32	0.29	0.36	0.26	0.3	0.29	0.42	0.34		0.29	0.26	0.31	0.37	0.29	0.32	0.29	0.3	0.29	0.25	0.66	0.63	0.96	0.68	1.1	0.26
SR	3.4	1.1	0.49	1.2	0.92	0.84	2.9	1	0.97	2.3	1.1	0.61	0.34	0.81	0.93	0.74	2.6	1.2		0.8	0.69	1.5	2.3	0.44	0.58	0.68	0.99	0.95	0.51	2.2	1.4	1.2	1.5	1.6	0.81
ZR	0.81	0.84	0.68	0.82	0.94	0.38	0.65	0.64	0.49	1.2	0.74	0.33	0.3	0.52	0.54	0.71	0.53	0.2		0.51	1.7	0.58	0.61	0.44	0.47	0.63	0.34	0.39	0.46	1.2	0.75	1	0.87	1.1	0.57
MO	1.5	0.77	1.6	0	1.2	1.4	0	0	0	0	1.1	1.5	1.8	3.2	0	1.7	0	0		2.4	2.8	1.5	1.7	1.5	1.7	0	1.9	0	2	0	0	2.2	0	0	1.4
BSO4			2200									2500		4400				4500	4300					1900	4800					2100		3200			
CLM			150									95		540				320	280					33	140					65		200			
NO2M			21									58		28				56	220					34	34					52		28			
NO3M			420									460		2300				730	520					190	6900					460		420			
NH4I																			1500																
NH3I																			1500																
SO2I10			940									2000		15000				3900						3600	1400					1900		4300			
SO2I25	4100	4500		3800	4500	1300	15000	4500	6200	8200	5200				3500	5200	5700			3900	1200	3800	5500			1600	15000	13000	4000		3100		2600	3300	5500
OCLT			260									1000		490				340						300	770					980		180			
OCHT			1600									5800		2500				1700						1500	4900					5900		1800			
ECLT			170									760		810				250						650	1200					1000		310			
ECHT			120									670		230				300						440	260					770		180			

Equation 6-1 is based on the assumption that the sulfate aerosol is fully neutralized by ammonium. Measurements of S (by XRF) and NH_4^+ (by AC) from the IMPROVE monitors during the summer intensive sampling period at Meadview indicated that the average aerosol molar ratio of $NH_4^+/SO_4^{2-} = 1.8 \pm 0.2$. For the most acidic sample (8/28/92 0700) the ratio $NH_4^+/SO_4^{2-} = 1.4$, and equation 6-1 overestimates the partially ammoniated sulfate mass by ~ 8%. The degree of neutralization of sulfate may have a larger effect on the aerosol's capacity to absorb water. Acidic aerosols absorb more water than neutralized aerosols at the same RH (Malm et al., 1998).

Table 6-5 Row heading definitions for Tables 6-1 through 6-4.

Abbreviation	Description
MF	Fine Mass
BAP	Particle optical absorption
M10	PM_{10} Mass
H	Hydrogen
NA	Sodium
MG	Magnesium
AL	Aluminum
SI	Silicon
P	Phosphorus
S	Sulfur
CL	Chlorine
K	Potassium
CA	Calcium
TI	Titanium
V	Vanadium
CR	Chromium
MN	Manganese
FE	Iron
NI	Nickel
CU	Copper
ZN	Zinc
AS	Arsenic
PB	Lead
SE	Selenium
BR	Bromium
RB	Rubidium
SR	Strontium
ZR	Zirconium
MO	Molybdenum
BSO4	Sulfate (Ion Chromatography)
CLM	Chloride
NO2M	Nitrite
NO3M	Nitrate
NH4I	Ammonium (Teflon)
NH3I	Ammonia from Ammonium (impregnated filter)
SO2I10	Sulfur Dioxide (impregnated filter) PM_{10}
SO2I25	Sulfur Dioxide (impregnated filter) $PM_{2.5}$
OCLT	Organic Carbon (Low Temp)
OCHT	Organic Carbon (High Temp)
ECLT	Elemental Carbon (Low Temp)
ECHT	Elemental Carbon (High Temp)

It should be noted that the IMPROVE sampler does not use an ammonia denuder to protect the acidic particles (collected on the Teflon filter) from acid neutralization. In addition, no precautions were taken to protect the samples during transport and storage. Thus, the

ammonium/sulfate ratio reported above may be positively biased. To date, denuder/filter pack techniques have been used to measure particle acidity and other ionic species (Koutrakis et al., 1992). The samplers consist of 3 components: (1) a $PM_{2.5}$ inertial impactor to remove coarse particles, (2) a diffusion denuder to remove gaseous ammonia from the air sample, and (3) a Teflon filter to collect fine particles.

Differences between the measured fine mass and the sum of the component concentrations above were classified as the unknown fraction. The unknown fractions may be composed of water, salt (NaCl), or other compounds not measured in the suite of chemical analyses. A negative unknown fraction indicates that the sum of the components exceeded the measured mass.

The molecular to carbon mass ratio of 1.4 applied to organic carbon to estimate the total mass of organic compounds may not be appropriate for all types of aerosol. The value was originally derived from measurements collected predominantly in the Los Angeles area. It has been hypothesized that the organic compounds in remote areas are more thoroughly oxidized and that the ratio should be higher than 1.4 (Hegg et al., 1997; Turpin et al., 1997). Better characterization of organic aerosols is needed to resolve this issue, however it is possible that some of the unknown fraction of the aerosol is organic. (Further discussion of these points is provided by Andrews et al., 1999).

The average aerosol chemical component concentrations are summarized in Figure 6-1 and Figure 6-2 for the winter and summer intensive periods. At Hopi Point, Meadview and San Gorgonio in the winter, the negative unknown component indicates that the calculated mass was larger than the measured mass. Component concentrations for each sample were calculated prior to averaging the component concentrations over the intensive sampling period. The figures indicate that summertime fine mass concentrations in the region were between 2 and 3 times greater than the winter concentrations. Ammonium sulfate was a large component of the fine mass aerosol in the region. Organic carbon was the second largest component representing a moderate to large fraction of the fine mass. At most sites, ammonium nitrate, soil, and elemental carbon each contributed a minor fraction to the aerosol mass. San Gorgonio is an exception in that ammonium nitrate accounted for a large fraction of fine mass. The relative contribution of each component did not change substantially from winter to summer across the network however the composition at some individual sites did change. It is notable, that the $PM_{2.5}$ is composed of a variety of components and that the composition at all sites is not dominated by a single component.

Based on IMPROVE data, at Meadview, ammonium sulfate accounted for 47 % and 41 % of the measured fine mass in the winter and summer, respectively. The next largest component was organic compounds which composed 40% of the fine mass in winter but only 11 % of the measured fine mass in the summer. Soil occupied 9 and 11 % of the fine mass at Meadview during the winter and summer. Ammonium nitrate and elemental carbon were minor components. Similar fine aerosol chemical profiles and seasonal patterns were also observed at Hopi Point on the south rim of the Grand Canyon and at Bryce Canyon in southern Utah.

The concentrations of particulate organic material determined using the BOSS denuder were over twice those determined from IMPROVE results. These results indicate that organic material averaged 54 %, ammonium sulfate 29 %, ammonium nitrate 4 %, soil 10 % and soot 2

% of the fine particulate mass at Meadview. The average concentration of fine particulate material, 7.2 µg/m^3, was comparable to the average coarse (PM_{10} - $PM_{2.5}$) particle concentration of 8.9 μg/m^3.

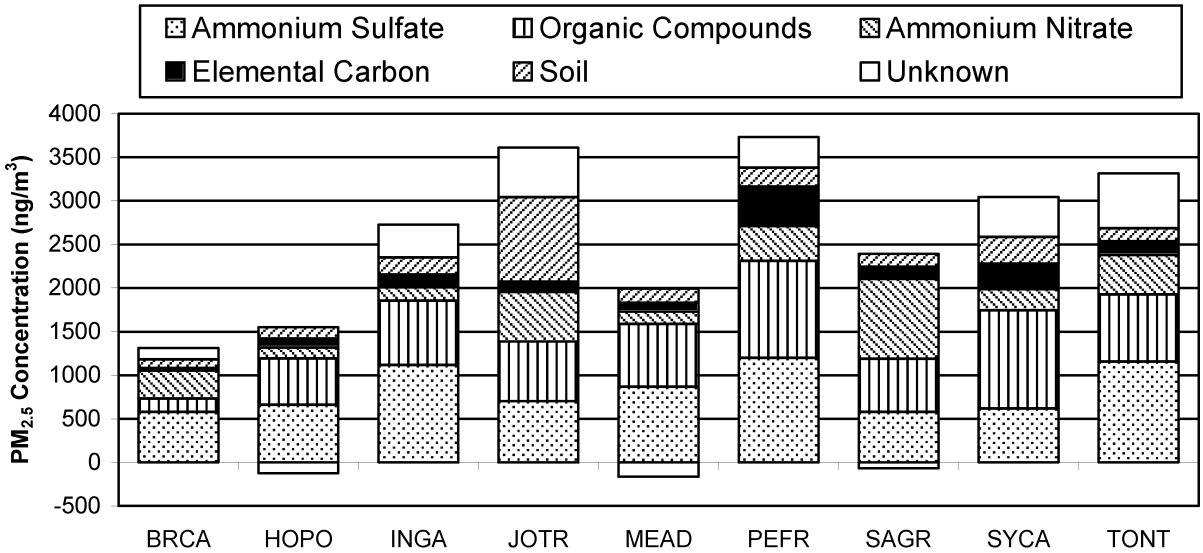

Figure 6-1 Wintertime average $PM_{2.5}$ composition at sampling sites within the Project MOHAVE study area.

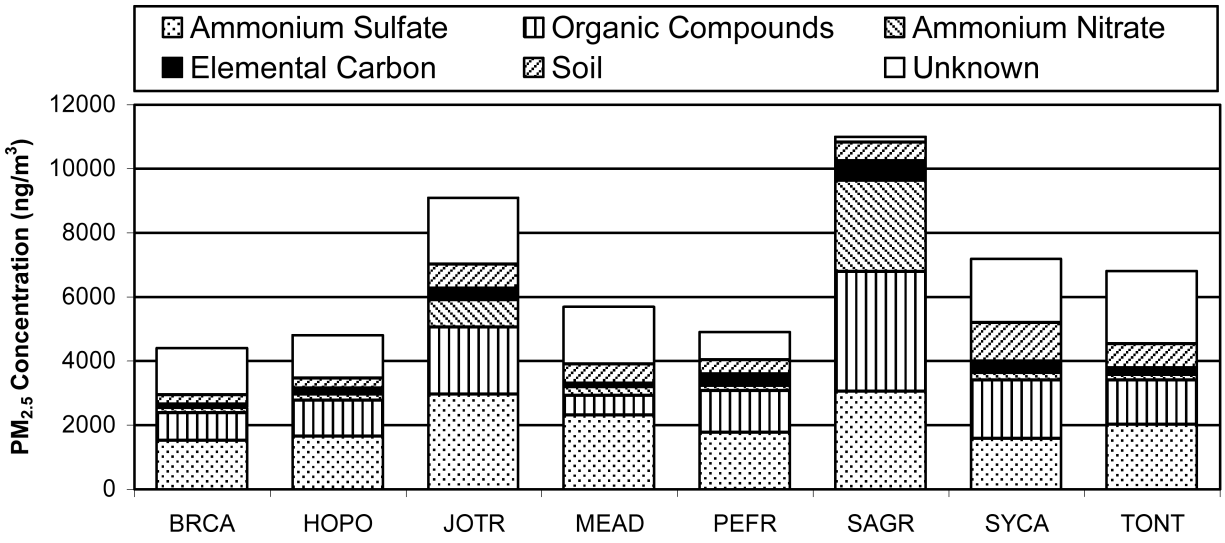

Figure 6-2 Summertime average $PM_{2.5}$ composition at sampling sites within the Project MOHAVE study area.

The two California sites Joshua Tree and San Gorgonio had higher total $PM_{2.5}$ levels than the other sites with carbon measurements. Ammonium nitrate was a substantial component (~20%) of the average $PM_{2.5}$ at San Gorgonio. The proximity of this site to Los Angeles suggests that polluted air from the city frequently impacts this location. At Joshua Tree in the winter time, soil accounts for approximately 27% of the fine mass which is a higher fraction than observed at any

of the other sites in winter or summer. A more detailed analysis of the summer and winter aerosol composition throughout the network is provided by Sisler and Malm (1997) and Gebhart and Malm (1997)

Using the complete speciated data set from the sites where organic and elemental carbon were measured, maps of the average component composition of the $PM_{2.5}$ aerosol were produced. Figure 6-3 and Figure 6-4 show pie charts of the chemical composition of the measured $PM_{2.5}$ during the winter and summer field seasons. The sizes of the pie charts increase with greater average aerosol concentration but are not directly proportional to the concentration. For example Bryce Canyon and Meadview have lower average $PM_{2.5}$ concentrations and smaller pie charts than Petrified Forest and San Gorgonio. The unknown component was not plotted.

The maps show the spatial gradients of the aerosol concentrations for sites with complete speciation. During the winter, higher $PM_{2.5}$ was observed in the southeast and southwest: in the summer, concentrations were highest in the southwest. (Note: Las Vegas Wash had the highest fine mass concentration during the winter intensive study.) In the Grand Canyon region (Meadview, Hopi Point, and Indian Gardens) during both winter and summer, sulfate and organic compounds are the largest components of the fine mass aerosol. This pattern is reflected at all other sites except for Joshua Tree, which had high concentrations of fine soil in the winter.

6.2 Temporal and Spatial Variation of Contributions to Extinction

The preceding section summarized the median, mean and maximum concentrations of chemical components observed throughout the MOHAVE network. The present section examines the daily variability of components at Meadview, the main receptor site.

The apportionment of total extinction into contributions from individual particle fractions raises a number of conceptual subtleties and technical difficulties (White, 1986; Sloane, 1986; White, 1990; Lowenthal et al., 1995; McMurry et al., 1996; Malm and Kreidenweis, 1997; and Malm, 1998). Some attributions are straightforward, like the contribution from scattering by gases. Some attributions are straightforward theoretically but very sensitive to measurement uncertainties, like the contributions from particle absorption, and scattering by large particles. And some attributions are ambiguous conceptually: there is no consensus that it is even meaningful to speak of the contribution from one chemical constituent of a mixed particle. Nonetheless, there is general agreement that some chemical components have more impact on total extinction than others do at similar mass concentrations

An indication of the relative importance of various particle components for visibility can be given by weighting their mass concentrations to approximate their optical effectiveness. The weighting coefficients should in principle vary from sample to sample, reflecting variations in components' distributions with respect to particle size and other factors. Such information is not generally available, although Malm and Kreidenweis (1997) were able to estimate sample-specific ammonium sulfate scattering ranging from 1.5 to 4.0 m^2/g over the summer intensive period. MOHAVE participants accordingly selected the following uniform calculation as illustrative, while recognizing its limitations:

$$b_{ext} = 2 \cdot f(RH) \cdot [(NH_4)_2 SO_4] + 3 \cdot f(RH) \cdot [NH_4 NO_3] + 4 \cdot [OMC] + 10 \cdot [EC] + [Soil] + 0.6 \cdot [CM] + 10.6 \qquad (6\text{-}6)$$

In Equation 6-6, total extinction (b_{ext}) and the constant (10.6) Rayleigh contribution from gases have units of Mm^{-1}. Concentrations are in $\mu g/m^3$, and the coefficients have units of m^2/g.

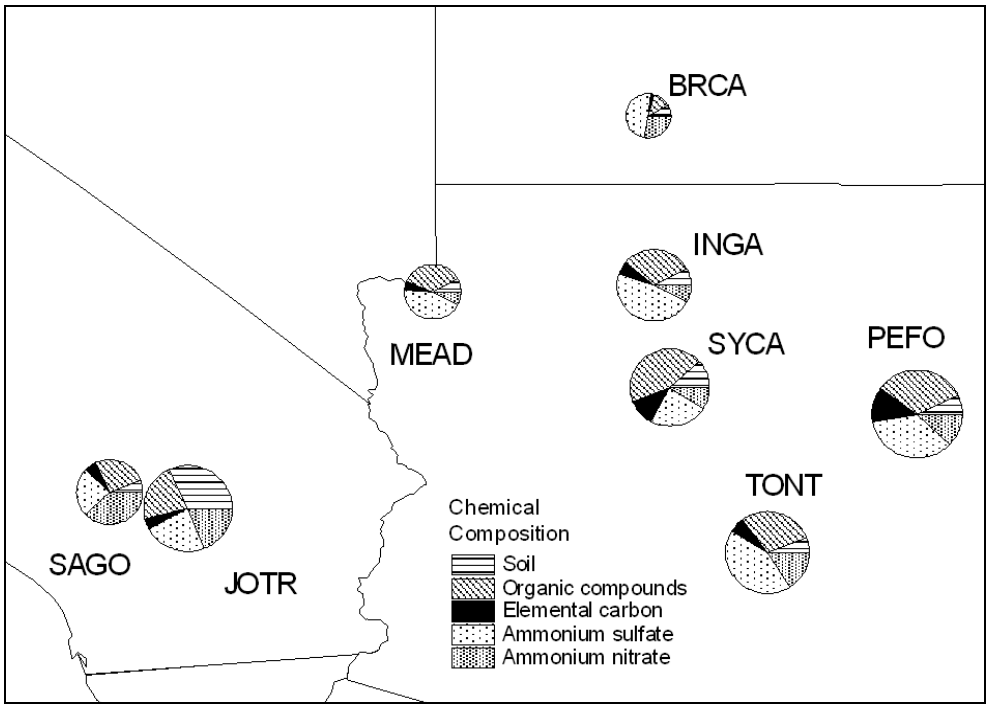

Figure 6-3 Wintertime average spatial distribution of chemical components.

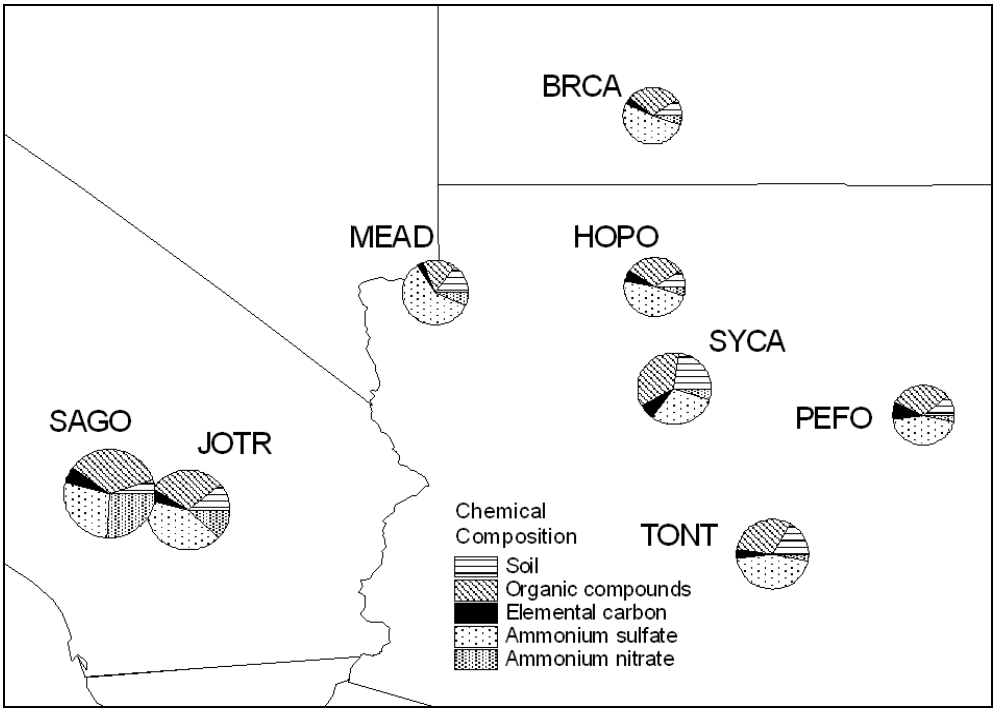

Figure 6-4 Summertime average spatial distribution of chemical components.

Components are as defined in equations 6-1 through 6-5 with the addition of coarse mass, [CM] = PM_{10} - $PM_{2.5}$. The *f*(RH) term is an empirical factor that accounts for the hygoscopicity of the sulfate and nitrate aerosols. As the humidity increases, the hygroscopic aerosols absorb water vapor and increase in size. Under normal conditions, this increases the aerosol's ability to scatter light in the visible spectrum. The values of *f(RH)* were derived using a particle growth model coupled with sulfate size distribution data from Meadview (Malm, 1998). The specific scattering of sulfate (2 m^2/g) is a result of Mie calculations using DRUM and MOUDI sulfur size distribution data and external mixing (Malm, 1998). Each of the terms in this equation represents the portion of light extinction due to sulfate, nitrate, organic compounds, elemental carbon, soil, coarse particles, and Rayleigh scattering. Notice that the use of elemental carbon to represent particle absorption may be the cause of the calculated extinction being systematically less than transmissometer extinction (see Section 5.4).

Using the IMPROVE aerosol chemical speciation and relative humidity data from Meadview, the relative components of light extinction ther can be estimated using Equation 6-6. For each 12 hour IMPROVE aerosol sample, the total extinction was calculated using Equation 6-6. The average and standard deviation of the component fraction of total extinction are plotted in Figure 6-5. On average, for both winter and summer, the largest single component of light extinction at Meadview is scattering. The remaining components comprise a larger fraction of the total extinction during the summer than during the winter since total light extinction is higher in the summer. The second largest component based on Equation 6-6 is organic compounds in winter (15%) and coarse mass in summer (16%). Sulfate particles from all sources are estimated to be responsible for 13% and 18% of the total light extinction in the winter and summer, respectively. The combined estimated contributions of fine soil, elemental carbon, and ammonium nitrate account for ~10% of the light extinction in both summer and winter.

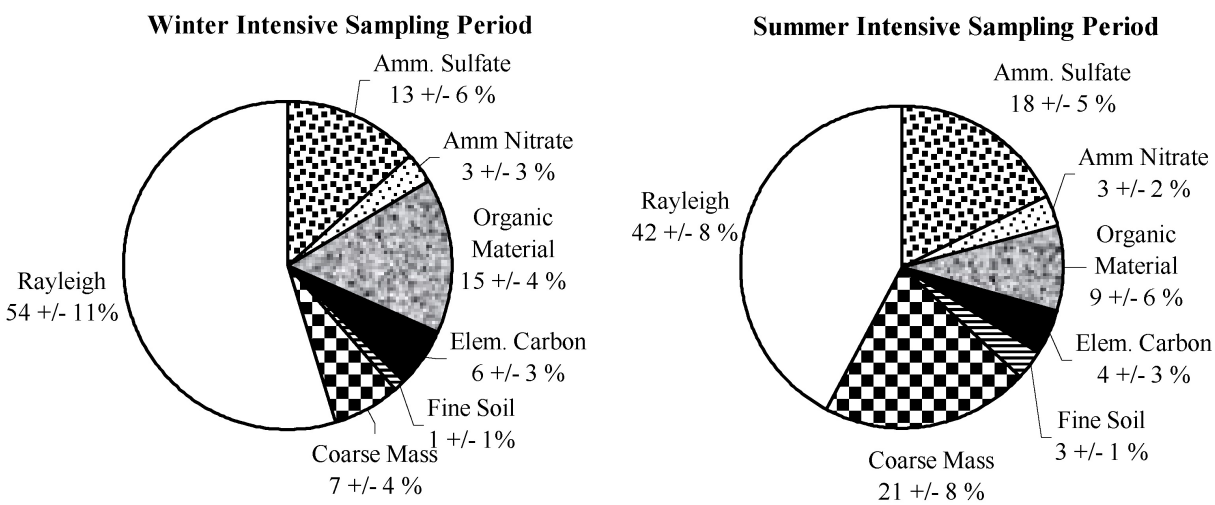

Figure 6-5 Seasonally averaged relative light extinction components at Meadview.

The concentration of fine particulate organic material determined using the BOSS denuder sampler was much smaller than that of the organic material retained on the IMPROVE filter. As a result, if the denuder results were substituted into equation 6-6, the relative fraction of organic

compounds to light extinction would increase by about 50% compared to the results shown in Figure 6-5.

The calculated extinction time series based on IMPROVE data for each sample collected during the intensive periods are shown in Figure 6-6 and Figure 6-7. On the left side of the figures are the relative contribution of each component to light extinction. On the right side of the figures are the absolute contributions to extinction. The total light extinction measured by the transmissometer is also shown in the right panels. Transmissometer data is only shown when there are 10 or more valid measurements within the 12 hour sampling period.

During the winter intensive, the calculated extinction is consistently less than the observed extinction. This is also true in the summer with the exception of the 7/21/92 0700 and 8/1/92 1900 samples. Coarse mass concentrations during these sampling periods were higher than the remaining periods from the summer intensive. It is possible that local sources near Meadview were producing coarse particles that would have impacted visibility on a local scale yet had negligible impact on extinction along the sight path of the transmissometer.

The average measured extinction was larger than the average calculated extinction during the winter and summer intensive periods by 9 ± 5 Mm^{-1} (31%) and 8 ± 6 Mm^{-1} (23%), respectively. Possible explanations for this discrepancy between calculated and measured extinction include any combination of the following:

- Equation 6-6 does not account for light absorption due to organic carbon species evolved at high temperatures by TOR analysis and fine soil particles (Malm et al., 1996 and Huffman, 1996).

- The mass of organic material may be under represented due to an inappropriate choice of the mass to carbon ratio in equation 6-3 (Hegg et al., 1997; Turpin et al., 1997).

- The transmissometer measurements may be larger than the true extinction due to an incorrect value for the effective lamp strength caused by problems with transmissometer alignment or calibration. (White et al., 1993).

6.3 Frequency of Different Atmospheric Constituents' Contribution to Different Levels of Haze

Using the simplified extinction Equation 6-6, the relative component contributions to extinction can be calculated at Meadview during the summer and winter intensive sampling periods. The results are displayed as frequency distributions of extinction budget contributions (Figure 6-8 and Figure 6-9). The frequency distributions indicate the potential for a single component to dominate the light extinction budget.

Highest winter sulfate contributions to extinction were ~30% for the 2/7/92 700 and 2/8/92 700 samples. This was the highest relative contribution to extinction during the winter intensive for all components except Rayleigh scattering.

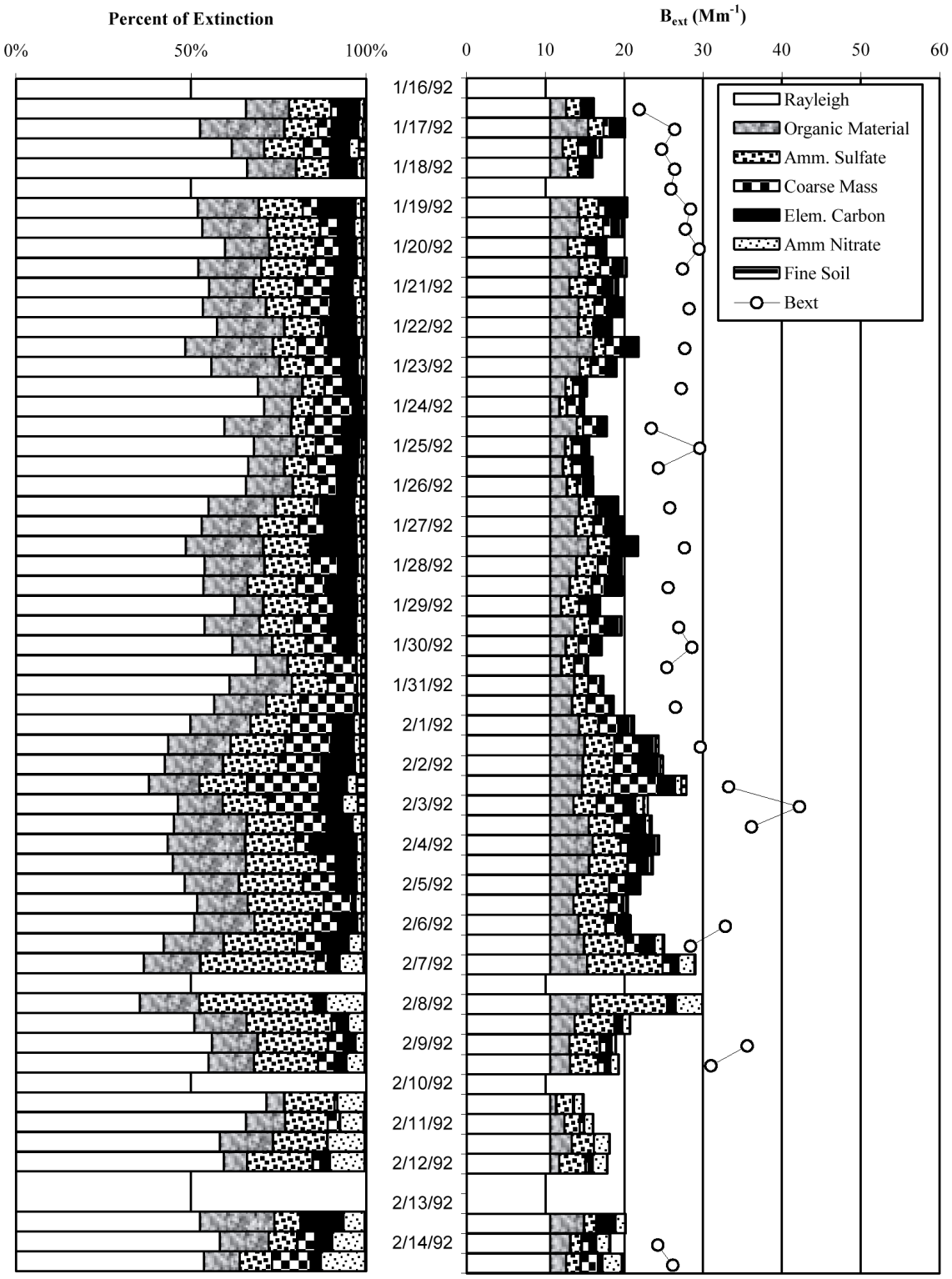

Figure 6-6 Wintertime relative (left panel) and absolute (right panel) calculated extinction at Meadview. The measured extinction from the transmissometer is shown as the open circles on the right panel.

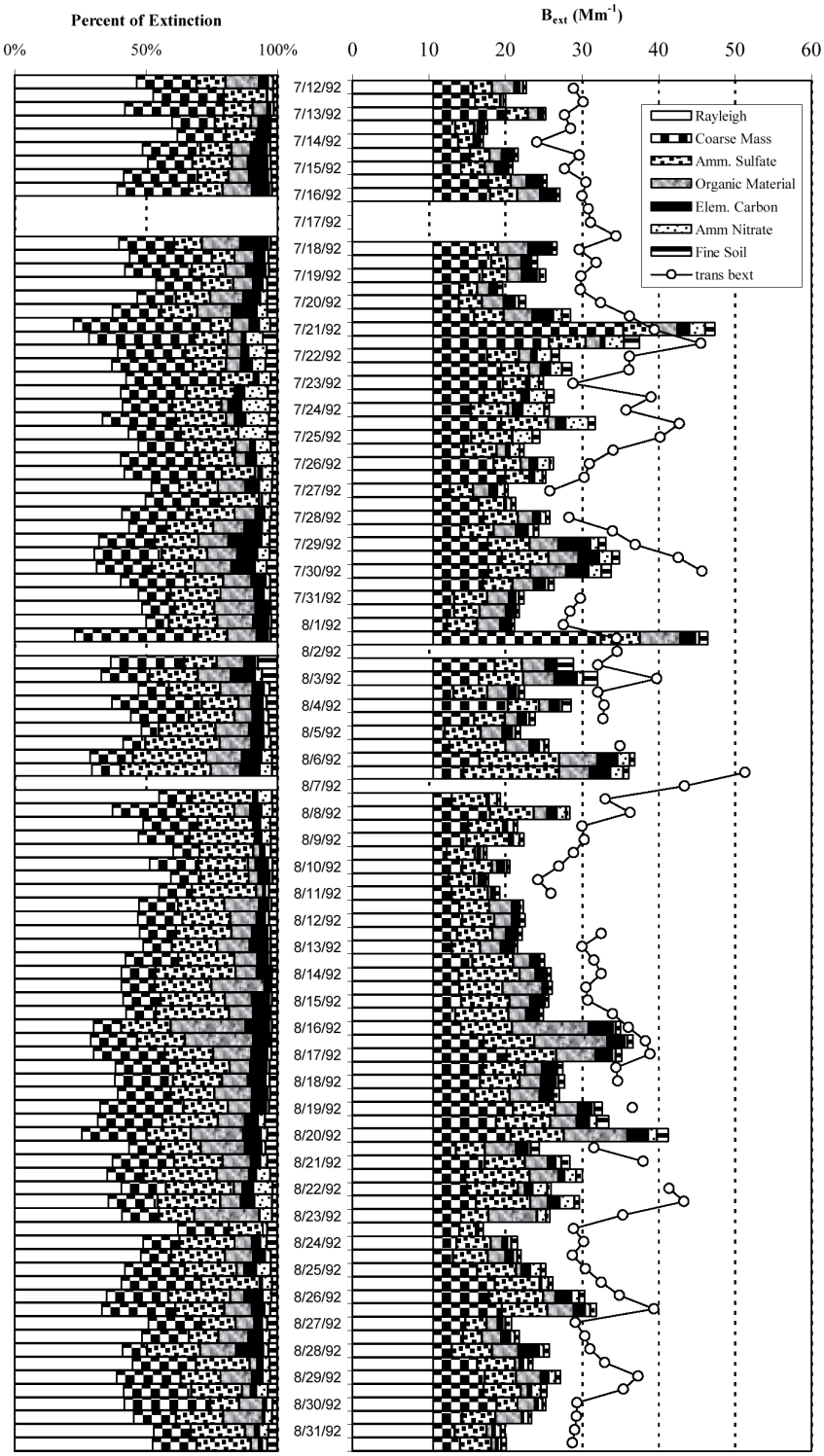

Figure 6-7 Summertime relative (left panel) and absolute (right panel) calculated extinction at Meadview. The measured extinction from the transmissometer is shown as the open circles on the right panel.

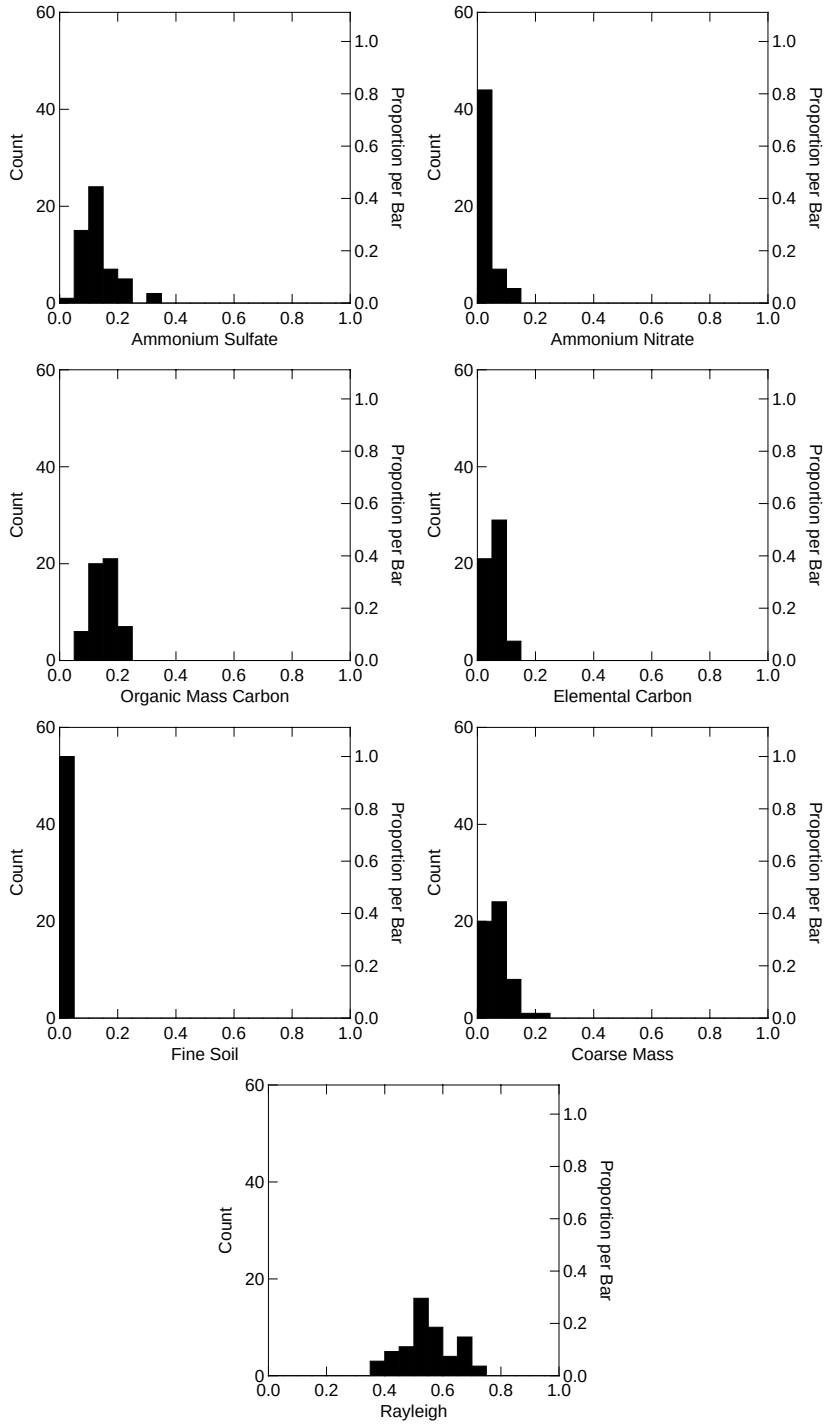

Figure 6-8 Winter relative chemical contribution frequency distribution to light extinction at Meadview based on IMPROVE data. The axis labeled "Count" represents the number of observations and the axis labeled "Proportion per Bar" represents the fraction of all observations within the bin.

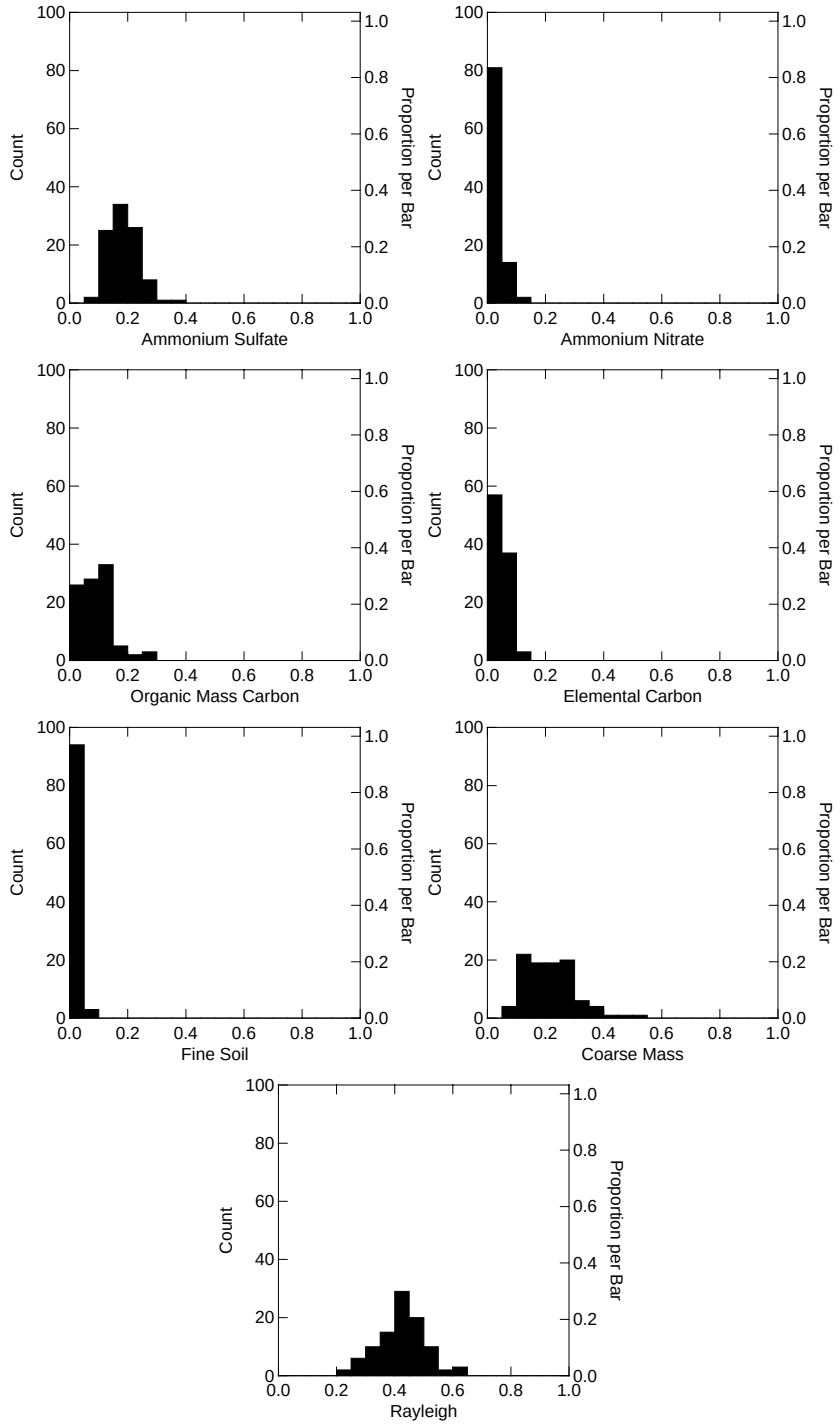

Figure 6-9 Summer relative chemical contribution frequency distribution to light extinction at Meadview based on IMPROVE data. The axis labeled "Count" represents the number of observations and the axis labeled "Proportion per Bar" represents the fraction of all observations within the bin.

During the summer intensive, the maximum estimated sulfate extinction accounted for 35% of the calculated extinction on 8/6/92 1900. Organic compound are estimated to have contributed a

maximum of 28% of the extinction during the 8/16/92 700 sample. On 7/21/92 700, equation 6-6 predicts that coarse mass contributed a maximum of 53% of the light extinction. For these three sampling periods, different components were the largest estimated contributors to extinction. Thus, complete control of the sources of a single extinction component would not have the same impact on light extinction for all days.

The figures also show that during the intensive sampling periods, fine soil never accounted for more than 10% of the light extinction. In addition, ammonium nitrate and elemental carbon never accounted for more than 15% of the light extinction.